Desalination and Water Treatment
www.deswater.com
doi: 10.5004/dwt.2023.29368

287 (2023) 245–253
March

Removal of eosin yellow from wastewaters by the commercial anion exchange membrane BI

Khalida Parveen[a], Shagufta Zafar[a], Muhammad Imran Khan[b,*], Ramsha Anwer[c], Abdallah Shanableh[b]

[a]*Department of Chemistry, The Government Sadiq College Women University, Bahawalpur 63000, Pakistan, emails: khalidap690@gmail.com (K. Parveen), shg_zf@gscwu.edu.pk (S. Zafar)*
[b]*Research Institute of Sciences and Engineering, University of Sharjah, Sharjah 27272, United Arab Emirates, email: raoimranishaq@gmail.com/mimran@sharjah.ac.ae (M.I. Khan), shanableh@sharjah.ac.ae (A. Shanableh)*
[c]*School of Economics, Bahauddin Zakariya University, Multan 60800, Pakistan; email: ramshaanwer04@gmail.com*

Received 15 November 2022; Accepted 4 February 2023

ABSTRACT

This article reports usage of the commercial anion exchange membrane BI as extraordinary adsorbent for the removal of eosin yellow from wastewater at room temperature. The dependence of percentage removal of eosin yellow on operating parameters was explored. The eosin yellow percentage removal was enhanced from 17% to 98%, 3% to 99.65% and 81% to 96% with increase in contact time, mass of anion exchange membrane BI and temperature while decreased from 95% to 31% with increase in initial concentration of eosin yellow. Experimental data was explored by employing non-linear adsorption kinetics models and non-linear adsorption isotherms. Adsorption kinetics study showed that eosin yellow adsorption onto anion exchange membrane BI fitted to non-linear pseudo-second-order model. Moreover, eosin yellow adsorption onto anion exchange membrane BI followed non-linear Langmuir isotherm with lower value of chi-square test ($\chi^2 = 3.442 \times 10^{-11}$). Thermodynamics study represented that eosin yellow adsorption was an endothermic process.

Keywords: Eosin yellow; Endothermic process; Anion exchange membrane; Adsorption; Non-linear isotherm

1. Introduction

Each year, a huge amount of wastewater is produced by households and modern manufacturing processes [1]. Water is most significant natural resource. There are now serious water shortages in several places throughout the world [2]. Water quality is seriously affected by human activities particularly industrial activities. When one or more contaminants that may negatively affect the water are released into it, it is considered to be polluted. These substances have the potential to affect the environment, people, animals and their ecosystems. Nowadays, water contamination is a global problem. Water pollution and contamination cause deaths and diseases throughout the world.

The first contaminant found in wastewater is color and it is extremely apparent and unwanted even when water contains just a little amount of dyes [3]. Any undesired addition of chemical compounds to water sources pollutes the water and makes it unfit for human usage. Dyes are one of the most hazardous poisons introduced into the environment among the many pollutants [4]. Around 4000 years ago organic dyes were first used. Industries including textiles, cosmetics, food and paper printing are employing dyes. The main consumer of dyes is the textile sector [5]. Textile

* Corresponding author.

industries especially paper and plastic industries utilize dyes for their goods [6]. Textile industry dumps massive amounts of colors into the environment. This is bad for the ecology and especially for groundwater [7]. Due to their extensive usage, durability and negative consequences synthetic dyes represent a serious concern to the environment and health of human when they are present in water and sewage [8]. Consequently, it is essential to remove dyes from polluted water by applying some suitable process.

To date a lot of methods such as advance oxidation electrooxidation, processes (AOPs), flocculation and coagulation, adsorption, membrane process and biological degradation were employed for decoloration and sewage-derived dye degradation [9–12]. Adsorption is most useful method for color because of its ease of usage, high efficiency and simplicity of design as well as the availability of a variety of adsorbents [13,14].

For the removal of heavy metals and dyes from wastewater, researchers used a variety of adsorbents such as activated clay, zeolites activated carbons, bio-nanocomposite (Alg-Cst/Kal), curcuma caesia-based activated carbon, Ag doped MnO_2-CNT nanocomposite, bimetallic-carbon nanocomposite, activated slag and nanocomposite films [15–39]. Currently, all the adsorbents employed for the removal of dyes and heavy metal ions based on the interaction of the adsorbate with the functional groups of the adsorbents [40]. As a result, having a wide surface area of the substrate and numerous adsorption sites contribute significantly to the effectiveness of the membranes' adsorption process for removing contaminants from wastewater [14,41]. Commercial anion exchange resins showed exceptional absorptivity and well-proven effective modification properties for the removal and recovery of reactive colorants [15,42]. Their packed-bed procedures would experience special defects because of the anion exchange resins' particle shape. For the purpose of removing methyl violet 2B from an aqueous solution two distinct types of ion exchange membranes including the ICE450 and P81 were used [43]. The anion exchange membranes from an aqueous solution were also used to extract cibacron Blue 3GA [43]. In addition to resolving the technical issues with packed-bed operation it also exhibits the ability to easily scale up by simply stacking numerous membranes or using a huge membrane area. As a result, the ion exchange membrane was a wise choice as an adsorbent for industrial applications.

This effort revealed eosin yellow (EY) adsorption from wastewater onto commercial anion exchange membrane (AEM) BI at room temperature. The consequence of contact time, AEM BI mass, initial concentration of EY, and temperature on the EY percentage elimination was explored. The kinetics of EY adsorption onto AEM BI was investigated using a non-linear adsorption kinetics model. Also, non-linear isotherms were used to elucidate EY adsorption. Adsorption thermodynamics for EY was also discussed. The environmental applicability of AEM BI was also discussed.

2. Experimental set-up

2.1. Adsorbent

Chemjoy Membrane Co., Ltd., Hefei, Anhui, China, provided commercial AEM BI, which was used as adsorbent. It was made up of quaternized poly(2,6-dimethyl-1,4-phenylene oxide) (QPPO) and polyvinyl alcohol. Its ion exchange capability is 0.55 mmol/g and water uptake are 42.7%.

2.2. Adsorbate

Eosin yellow (EY) a widely available anionic dye. It was utilized as an adsorbate. Its measured amount was dissolved into deionized water to create a stock solution of 1,000 mg/L. Further dilution of the stock solution yielded the necessary EY concentrations. EY chemical structure is shown in Fig. 1.

2.3. Batch adsorption of EY

Batch EY adsorption onto AEM BI from wastewater was conducted as described [43–51]. The contact time influence on EY adsorption was conducted at room temperature by shaking AEM BI (0.15) into measured volume of EY aqueous phase with original concentration of 50 mg/L at 200 rpm for 10, 20, 30, 40, 50 and 60 min. To determine optimum mass of AEM BI, varying amounts of AEM BI such as 0.015, 0.025, 0.030, 0.040, 0.07, 0.08, 0.09, 0.10, 0.125, 0.15, 0.175, 0.20 g were shaked at 200 rpm for 60 min into EY solution of 50 mg/L of measured volume. EY initial concentration effect was revealed by changing it from 10 to 175 mg/L using determined amount of AEM BI (0.15 g) into measured volume of EY solution for 60 min at room temperature. To study effect of temperature, we shaked measured amount of AEM BI (0.15 g) into measured volume of EY solution of determined initial concentration (50 mg/L) for 60 min at 200 rpm by varying temperature from 283 to 328 K. The EY concentration was recorded by using UV-VIS spectrophotometer (UV-2550, Shimadzu, Kyoto, Japan) by determining the absorbance of the supernatant at wavelength of 518 nm. The calibration curve was used to determine the EY content. EY adsorbed at time t was determined by means of Eq. (1).

$$q_t = \frac{C_o - C_t}{W} \times V \tag{1}$$

where C_o and C_t and C_o represent EY concentration at initial state and at time t, respectively. In the same way,

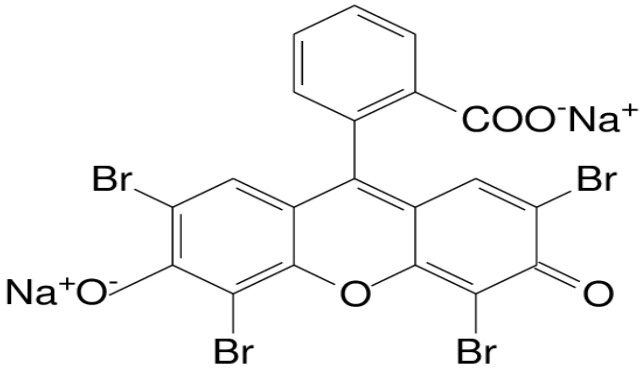

Fig. 1. Chemical structure of eosin yellow.

W and V stand for the corresponding weight of AEM BI and volume of the EY solution.

2.4. Adsorption isotherms

EY adsorption onto AEM BI was demonstrated by using non-linear two parameters isotherms (Langmuir, Freundlich, Dubinin–Radushkevich (D-R), Temkin) and three parameter isotherms (Redlich–Peterson, Hill and Sips) as follows.

2.4.1. Two parameters adsorption isotherms

Langmuir, Dubinin–Radushkevich, Freundlich and Temkin isotherms were used by non-linear method to investigate EY adsorption onto AEM BI.

Non-linear Langmuir isotherm model is given as [43]:

$$q_e = \frac{Q_m k_L C_e}{1 + K_L C_e} \tag{2}$$

where k_L and Q_m stand for the Langmuir constant (L/mol) and the Langmuir monolayer adsorption capacity (mol/g), respectively.

Non-linear Freundlich isotherm model is represented as [43]:

$$q_e = K_f C_e^{1/n} \tag{3}$$

where K_f and n are Freundlich parameters, C_e is the effluent concentration at equilibrium level of the system (mol/L) and q_e is the quantity of dye adsorbed at equilibrium point in the system (mol/g).

D-R model was utilized to distinguish between chemical and physical adsorption processes [43,52].

$$q_e = C_m \exp\left(-\beta\varepsilon^2\right) \tag{4}$$

The Polanyi potential is specified as ε;

$$\varepsilon = RT \ln\left(1 + \frac{1}{C_e}\right) \tag{5}$$

where T is the absolute temperature and R is the universal gas constant (kJ/mol·K). Mean energy can be determined by:

$$E = \frac{1}{\sqrt{2\beta}} \tag{6}$$

Temkin isotherm is given as [43]:

$$q_e = \frac{RT}{b_T} \ln\left(a_T C_e\right) \tag{7}$$

where a_T is the equilibrium binding constant that corresponds to the maximum binding energy and b_T is proportional to the heat of adsorption.

2.4.2. Three parameters adsorption isotherms

Hill, Redlich–Peterson and Sips are three parameter isotherm models that are empirical in nature and indicate adsorption capacity as a basic function of equilibrium concentration were utilized to reveal EY adsorption onto AEM BI [43].

Non-linear Hill adsorption isotherm is given as:

$$q_e = \frac{q_H C_e^{n_H}}{k_H + C_e^{n_H}} \tag{8}$$

Redlich–Peterson isotherm contains element of Freundlich and Langmuir isotherms which explain equilibrium on heterogeneous and homogeneous surfaces and multilayer adsorption. It possess three endowments such as a_{RP}, K_{RP} and g and is shown by as:

$$q_e = \frac{K_{RP} C_e}{1 + a_{RP} C_e^g} \tag{9}$$

Over a broad range of dye intensity molecules it is utilized to describe adsorption equilibrium. The range of the exponent g is from 0 to 1. when β = 1, the R-P equation becomes the Langmuir equation and when β = 0, it becomes the Henry's law [53].

Sips isotherm, which combines the Langmuir and Freundlich isotherms was developed to determine the heterogeneous adsorption process [54]. Non-linear Sips adsorption isotherm is expressed by:

$$q_e = \frac{K_S C_e^{\beta}}{1 + a_S C_e^{\beta}} \tag{10}$$

2.5. Adsorption kinetics

Non-linear pseudo-first-order and pseudo-second-order models were applied to explore adsorption kinetics for EY adsorption onto AEM BI.

2.6. Adsorption thermodynamic study

Thermodynamics of adsorption equations were used to investigate EY adsorption onto AEM BI:

$$\ln K_c = \frac{\Delta S^\circ}{R} - \frac{\Delta H^\circ}{RT} \tag{11}$$

$$K_c = \frac{C_a}{C_e} \tag{12}$$

$$\Delta G^\circ = \Delta H^\circ - T\Delta S^\circ \tag{13}$$

where R, K_c, ΔG°, ΔS° and ΔH° stand for the general gas constant, the equilibrium constant, the change in Gibb's free energy, the change in entropy (J/mol·K) and the change in enthalpy (kJ/mol), respectively.

3. Results and discussion

3.1. Effect of operating parameters on the EY removal

Fig. 2a indicates contact time's effect on the percentage elimination of EY from wastewater at room temperature. It was noted that percentage EY removal was increased with contact time. From Fig. 2a it is seen that removal of EY in initial stage was very rapid and increased continuously until equilibrium is attained. The rapid EY removal in initial stage was due to occurrence of several empty sites onto AEM BI [9,14]. Contrary, the decline in EY removal with passing time was associated to coverage of empty active sites onto the commercial AEM BI [9,10]. After 60 min finally equilibrium was achieved. The optimum time was used for further experiments.

Mass of adsorbent plays a vital part during adsorption process. The effect of mass of AEM BI on EY percentage removal of investigated at room temperature and attained results are represented in Fig. 2b. The EY removal was found to be increased from 2.85% to 99.65% with increase in AEM BI dosage 0.015–0.20 g. The EY removal enhancement with AEM BI dosage was due to increase in number of active sites onto AEM BI for EY adsorption [13,55]. As seen in Fig. 2b, the EY removal was rapid initially with enhancement in AEM BI dosage and then no huge enhancement in EY removal was noted with increase in AEM BI dosage from 0.15 g. Therefore, 0.15 g AEM BI (optimum dosage) was used in further research.

Effect of EY initial concentration on the percentage removal was explored by changing concentration from 50 to 200 mg/L and attained results are denoted in Fig. 2c. The EY percentage removal was found to be declined with increase in initial concentration of EY. The decrease in EY percentage removal was because of saturation of active sites due to higher initial concentration of EY [43,56].

Fig. 2d represents effect of temperature on EY percentage removal from wastewater. Results indicate that EY removal was increased with increase in temperature. The EY percentage removal was found to be increased from 81% to 96% with increase in temperature from 283 to 328 K. These finding represented that EY removal from wastewater was endothermic process. Further, the mechanism of EY adsorption onto AEM BI from wastewater is denoted in Fig. 3.

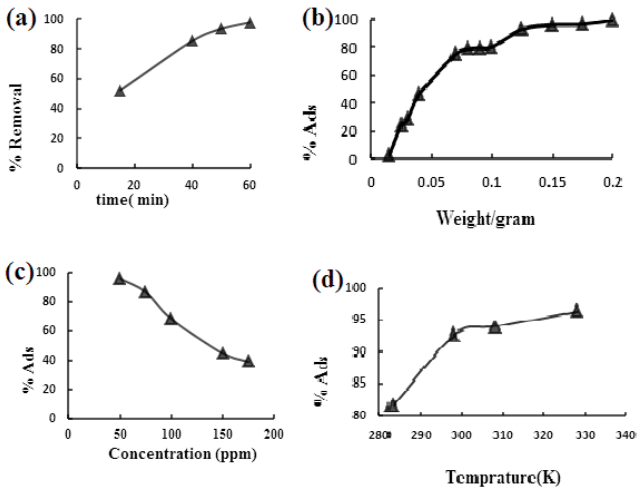

Fig. 2. (a) Effect of contact time, (b) BI membrane mass, (c) initial concentration, and (d) temperature on removal of eosin yellow from wastewater.

3.2. Adsorption kinetics

On the time-dependent adsorption data of EY onto AEM BI non-linear kinetic models including pseudo-first-order and pseudo-second-order were utilized. Using non-linear equations determine the kinetic parameters, IGOR Pro 6.1.2, Wave Metrices software was employed.

The Lagergren's pseudo-first-order kinetic model is represented as [57]:

$$\frac{dQ_t}{dt} = k_1\left(Q_e - Q_t\right) \tag{14}$$

The pseudo-second-order kinetic model is given as [58,59]:

$$\frac{dQ_t}{dt} = k_2\left(Q_e - Q_t\right)^2 \tag{15}$$

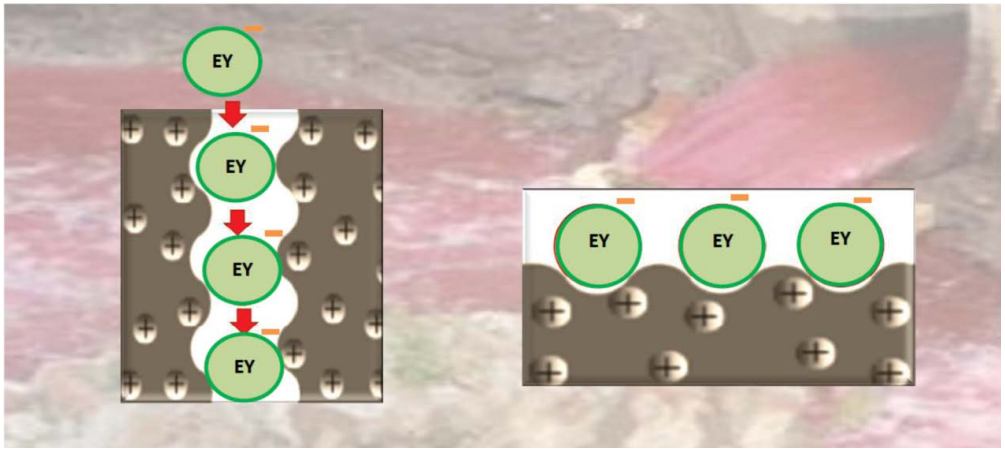

Fig. 3. Mechanism of eosin yellow adsorption onto anion exchange membrane BI from wastewater.

where Q_e is the amount of EY adsorbed at equilibrium (mg/g), t is time (min), Q_t is the quantity of EY adsorbed at time "t", k_1 is the rate constant of the pseudo-first-order model (g/mg·min), and k_2 is the rate constant of the pseudo-second-order model (g/mg·min). Non-linear pseudo-first-order model is given as:

$$Q_t = Q_e\left(1 - e^{-kt}\right) \tag{16}$$

Non-linear pseudo-second-order model is expressed as:

$$Q_t = \frac{k_2 Q_e^2 t}{1 + k_2 Q_e t} \tag{17}$$

Fig. 4 shows pseudo-first-order and pseudo-second-order kinetic model's non-linear graphs for the adsorption of EY onto AEM BI. The values of constants and theoretically calculated Q_e are given in Table 1.

Chi-square test 'χ^2' was used to calculate the best-fit of the kinetic equations using several models:

$$\chi^2 = \sum \frac{\left(Q_e - Q_{e,m}\right)^2}{Q_{e,m}} \tag{18}$$

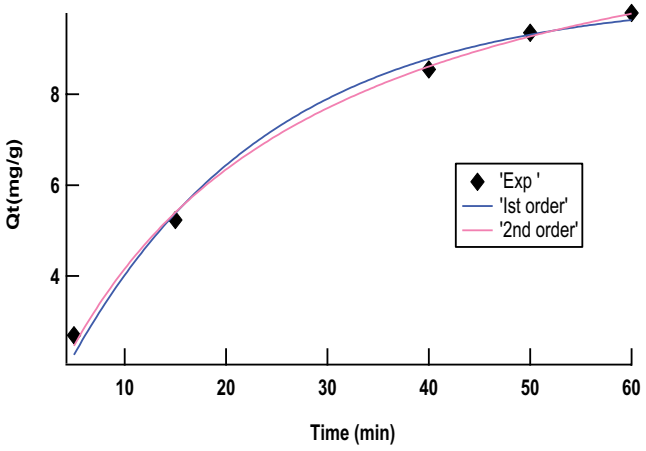

Fig. 4. Non-linear pseudo-first-order and pseudo-second-order models for eosin yellow adsorption onto anion exchange membrane BI.

Table 1
Measured values of non-linear pseudo-first-order and pseudo-second-order models parameters for eosin yellow adsorption onto anion exchange membrane BI.

Adsorption kinetics models	Measured parameters	
Pseudo-first-order model	q_e	10.12
	k_1	0.050
	χ^2	0.29
Pseudo-second-order model	q_e	13.41
	k_2	0.0035
	χ^2	0.093

k_1: min^{-1}; k_2: g/mg·min, q_e: mg/g.

where $Q_{e,m}$ is the equilibrium capacity determined by the model (mg/g) and Q_e is the equilibrium capacity measured using the experimental data (mg/g). The calculated values for 'χ^2' are provided in Table 1. Comparing model-derived data with experimental data typically reveals whether the data are similar in this case 'χ^2' would indicate a limited number and *vice versa*. The pseudo-second-order model appears to be more trustworthy for determining the kinetic constants for adsorption as evidenced by the computed lower values of the non-linear 'χ^2' test analysis of EY onto AEM BI.

3.3. Adsorption isotherms

Using both two and three parameter isotherm models, adsorption of EY onto AEM BI was revealed. Non-linear method was used for determination of adsorption isotherm's parameters. Igor Pro was utilized to reveal isotherm factors by non-linear regression WaveMatrices 6.2.1 software [43,60]. Non-linear chi-square test (χ^2) is a statistical method for determining the best fitting of adsorption data. The larger value represents variety in the experimental data whereas the lower value shows similarities between the EY experimental data [61].

3.3.1. Two parameters adsorption isotherms

Non-linear Langmuir isotherm for EY adsorption onto AEM BI is shown in Fig. 5. Measured values of Q_m and k_L are given in Table 2. EY adsorption onto AEM BI fitted to non-linear Langmuir isotherm as represented by the lower value of chi-square test (χ^2 = 3.442 × 10^{-11}). Fig. 5 shows non-linear Freundlich isotherm for EY adsorption and determined values of K_f and n are provided in Table 2. The lower value of chi-square test (χ^2 = 1.06 × 10^{-10}) showed that EY adsorption followed Freundlich isotherm model. Freundlich constant 'n' values between 2 and 10 indicate good adsorption, 1 and 2 suggest moderate adsorption, and less than 1 indicates poor adsorption [62,63]. Temkin isotherm for EY adsorption onto AEM BI by non-linear method is denoted Fig. 5 and calculated values of b_T and a_T are given in Table 2. The lower value of chi-square (χ^2 = 1.02 × 10^{-10}) represented that EY adsorption followed Temkin isotherm. D-R isotherm

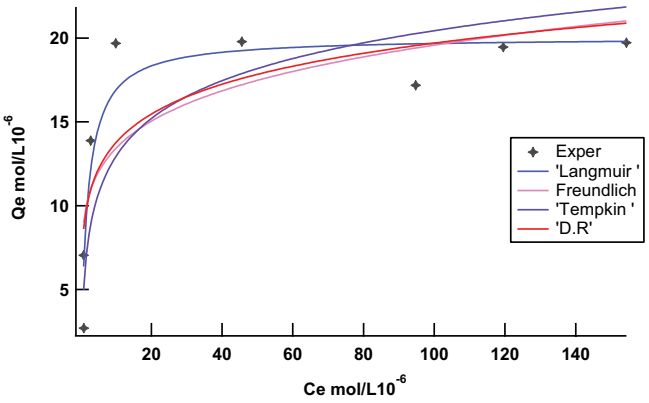

Fig. 5. Non-linear Langmuir, Freundlich, Temkin and Dubinin–Radushkevich isotherms for eosin yellow adsorption onto anion exchange membrane BI.

for EY adsorption onto AEM BI by non-linear method is depicted in Fig. 5. Measured value of mean adsorption energy (E) was 31.25 kJ/mol. It represented that EY adsorption followed chemical ion exchange adsorption mechanism onto AEM BI. The mean adsorption energy (E) in D-R isotherm plays a significant rule to distinguish between physical and chemical adsorption [43,63]. The value of E greater than 8 kJ/mol represented chemical ion exchange adsorption process whereas value of E below 8 kJ/mol showed physical adsorption process [43,63].

3.3.2. Three parameters adsorption isotherms

R-P model for EY adsorption onto AEM BI is represented in Fig. 6. Results denoted that R-P model with lower value of ($\chi^2 = 1.07 \times 10^{-10}$) explained EY adsorption onto AEM BI. Its measured factors are given in Table 3. Sips isotherm for EY adsorption is shown in Fig. 6 and measured Sips constants are shown in Table 3. The smaller value of ($\chi^2 = 3.412$) represented that Sips equation obeyed equilibrium data. Fig. 6 shows Hill isotherm for EY adsorption onto AEM BI and measured values of its factors are given in Table 3. The lower value of chi-square ($\chi^2 = 3.962 \times 10^{-11}$) showed that EY adsorption onto AEM BI followed Hill model.

Table 2
Determined endowment values for two parameters non-linear adsorption isotherms

Adsorption isotherms	Measured parameters	
Langmuir isotherm	Q_m	2.004×10^5
	k_L	5.38×10^5
	χ^2	3.442×10^{-11}
Freundlich isotherm	K_f	8.85×10^{-5}
	n	6.104
	χ^2	1.06×10^{-10}
Temkin isotherm	a_T	5.32×10^6
	b_T	7.53×10^5
	χ^2	1.02×10^{-10}
Dubinin–Radushkevich isotherm	Q_m	3.726×10^{-5}
	β	0.001
	χ^2	9.56×10^{-11}
	$E = 31.25$	

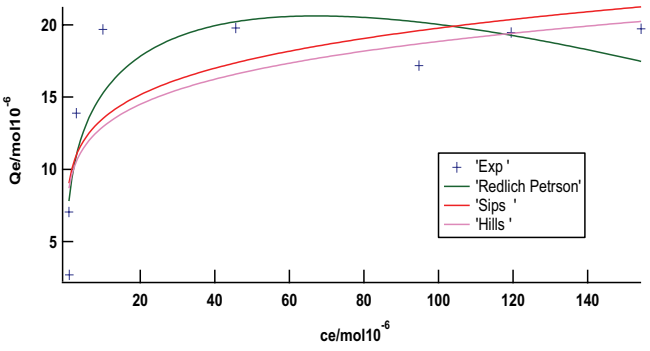

Fig. 6. The plots of three parameters adsorption isotherms for eosin yellow adsorption onto anion exchange membrane BI by non-linear method.

3.4. Adsorption thermodynamics

Fig. 7 indicates $1/T$ vs. $\ln K_c$ plot for EY adsorption onto AEM BI. Measured values of thermodynamics factors for EY adsorption are given in Table 4. The positive value of enthalpy ($\Delta H°$ = 20.837 kJ/mol) showed that EY adsorption onto AEM BI was endothermic process [64]. As shown in Table 4, the value of Gibb's free energy was negative for EB adsorption onto AEM BI denoting that EY adsorption was spontaneous and feasible process [12,13]. The enhancement in randomness at AEM BI–EY interface was noted

Table 3
Determined endowment values for three parameters non-linear adsorption isotherms

Adsorption isotherms	Measured parameters	
Hills isotherm	q_H	0.224
	n_H	0.165
	K_d	248.4
	χ^2	1.07×10^{-10}
Redlich–Peterson isotherm	a	7.360
	K	3.139
	G	1.1008
	χ^2	3.412
Sips	K_s	2.735
	B	0.899
	A_s	1.35×10^5
	χ^2	3.962×10^{-11}

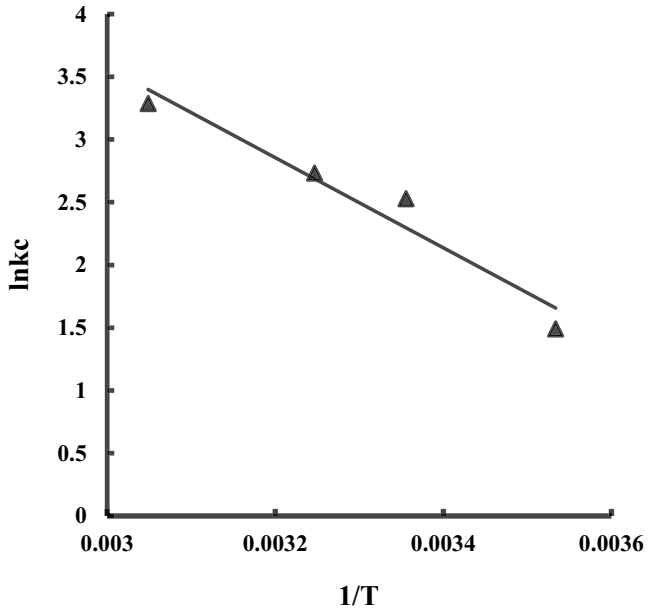

Fig. 7. Adsorption thermodynamics plot for eosin yellow adsorption onto anion exchange membrane BI.

Table 4
Determined values of entropy, enthalpy and Gibb's free energy for adsorption of eosin yellow on anion exchange membrane BI

Temperature (K)	$\Delta H°$ (kJ/mol)	$\Delta S°$ (kJ/mol)	$\Delta G°$ (kJ/mol)
283	20.837	0.090	–4.837
298			–6.197
308			–7.105
328			–8.919

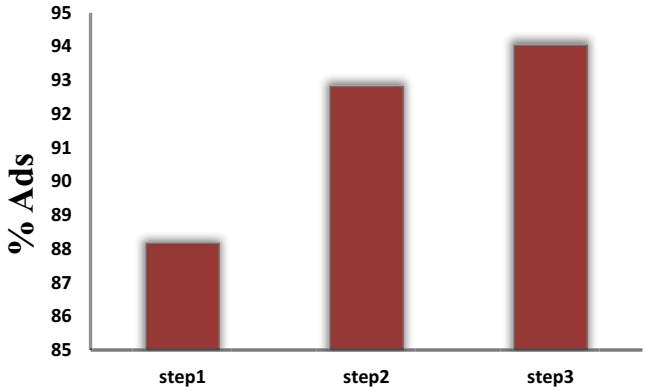

Fig. 8. Environmental applicability of anion exchange membrane BI.

due to positive value of entropy (0.090 kJ/mol) during EY adsorption onto AEM BI [64].

3.5. Environmental application

The dye was removed from a tap water sample to demonstrate the environmental applicability of AEM BI. The stock solution of EY was prepared in tap water. Then 30 mL of dye was taken along with optimum amount of adsorbent (AEM BI) 0.15 g and was kept on orbital shaker for optimum time. After that, the sample's absorbance was determined. Adsorption of 50 mg/L solution was up to 88% in first cycle and reached 94% in third cycle. These result implied the good applicability of AEM BI for EY adsorption. Attained results are shown in Fig. 8.

4. Conclusions

In this research, adsorption of EY from wastewater onto AEM BI was revealed at room temperature. The EY percentage removal was enhanced with contact time, AEM BI dosage and temperature while decline with increasing EY initial concentration. EY adsorption onto AEM BI followed non-linear pseudo-second-order kinetics. Moreover, adsorption of EY followed non-linear Langmuir adsorption isotherm. It was noted that EY adsorption was chemical ion exchange adsorption process with mean adsorption energy (E) value of 31.25 kJ/mol. Adsorption thermodynamic investigations represented that adsorption of EY onto AEM BI was a spontaneous and endothermic process. This work demonstrated the significant potential of AEM BI for its application in wastewater treatment.

Acknowledgements

The authors are highly thankful to Government Sadiq College Women University (GSCWU), Bahawalpur, Pakistan for financial support.

References

[1] M. Khan, M. Khan, S. Zafar, S. Hussain, Adsorption kinetics and thermodynamics study for the removal of anionic dye Eosin-B from aqueous solution by anion exchange membrane: adsorption kinetics and thermodynamics, Sch. J. Eng. Technol., 3 (2015) 741–749.
[2] J.N. Halder, M.N. Islam, Water pollution and its impact on the human health, J. Environ. Human, 2 (2015) 36–46.
[3] S. Gopi, A. Pius, S. Thomas, Enhanced adsorption of crystal violet by synthesized and characterized chitin nano whiskers from shrimp shell, J. Water Process Eng., 14 (2016) 1–8.
[4] H. Masood, S. Zafar, H. Rehman, M.I. Khan, H.B. Ahmadd, A. Naz, W. Hassan, M.H. Lashari, Adsorptive removal of anionic dyes in aqueous binary mixture by anion exchange membrane, Desal. Water Treat., 194 (2020) 248–258.
[5] S. El Harfi, A. El Harfi, Classifications, properties and applications of textile dyes: a review, Appl. J. Environ. Eng. Sci., 3 (2017) 00000–00003 N° 00003 (02017) 00311–00320.
[6] S. Rangabhashiyam, N. Anu, N. Selvaraju, Sequestration of dye from textile industry wastewater using agricultural waste products as adsorbents, J. Environ. Chem. Eng., 1 (2013) 629–641.
[7] C. Meziti, A. Boukerroui, Removal of a basic textile dye from aqueous solution by adsorption on regenerated clay, Process Eng., 33 (2012) 303–312.
[8] S. Caprarescu, A.R. Miron, V. Purcar, A.-L. Radu, A. Sarbu, D. Ion-Ebrasu, L.-I. Atanase, M. Ghiurea, Efficient removal of Indigo Carmine dye by a separation process, Water Sci. Technol., 74 (2016) 2462–2473.
[9] M.I. Khan, A. Shanableh, N. Nasir, S. Shahida, Adsorptive removal of methyl orange from wastewaters by the commercial anion exchange membrane EPTAC, Desal. Water Treat., 234 (2021) 245–254.
[10] M.I. Khan, J. Su, L. Guo, Development of triethanolamine functionalized-anion exchange membrane for adsorptive removal of methyl orange from aqueous solution, Desal. Water Treat., 209 (2021) 342–352.
[11] M.I. Khan, A. Shanableh, Adsorption of Rhodamine B from an aqueous solution onto NaOH-treated rice husk, Desal. Water Treat., 252 (2022) 104–115.
[12] S. Zafar, M.I. Khan, N. Elboughdiri, M.H. Lashari, A. Shanableh, S. Shahida, S. Manzoor, Adsorption performance of rice husk towards copper ions from wastewater, Desal. Water Treat., 258 (2022) 133–142.
[13] M.I. Khan, A. Shanableh, N. Elboughdiri, M.H. Lashari, S. Manzoor, S. Shahida, N. Farooq, Y. Bouazzi, S. Rejeb, Z. Elleuch, K. Kriaa, A. Rehman, Adsorption of Methyl Orange from an aqueous solution onto a BPPO-based anion exchange membrane, ACS Omega, 7 (2022) 26788–26799.
[14] M.I. Khan, A. Shanableh, J. Fernandez, M.H. Lashari, S. Shahida, S. Manzoor, S. Zafar, A. ur Rehman, N. Elboughdiri, Synthesis of DMEA-grafted anion exchange membrane for adsorptive discharge of Methyl Orange from wastewaters, Membranes, 11 (2021) 166, doi: 10.3390/membranes11030166.
[15] S. Karcher, A. Kornmüller, M. Jekel, Screening of commercial sorbents for the removal of reactive dyes, Dyes Pigm., 51 (2001) 111–125.
[16] V.K. Gupta, S.K. Srivastava, D. Mohan, Equilibrium uptake, sorption dynamics, process optimization, and column operations for the removal and recovery of malachite green

from wastewater using activated carbon and activated slag, Ind. Eng. Chem. Res., 36 (1997) 2207–2218.
[17] V. Gupta, Suhas, I. Ali, V. Saini, Removal of rhodamine B, fast green, and methylene blue from wastewater using red mud, an aluminum industry waste, Ind. Eng. Chem. Res., 43 (2004) 1740–1747.
[18] V. Gupta, I. Ali, V. Saini, T. Van Gerven, B. Van der Bruggen, C. Vandecasteele, Removal of dyes from wastewater using bottom ash, Ind. Eng. Chem. Res., 44 (2005) 3655–3664.
[19] V.K. Gupta, A. Mittal, V. Gajbe, J. Mittal, Removal and recovery of the hazardous azo dye Acid Orange 7 through adsorption over waste materials: bottom ash and de-oiled soya, Ind. Eng. Chem. Res., 45 (2006) 1446–1453.
[20] I. Šimkovic, J.A. Laszlo, A.R. Thompson, Preparation of a weakly basic ion exchanger by crosslinking starch with epichlorohydrin in the presence of NH_4OH, Carbohydr. Polym., 30 (1996) 25–30.
[21] K. Low, C. Lee, Quaternized rice husk as sorbent for reactive dyes, Bioresour. Technol., 61 (1997) 121–125.
[22] J.A. Laszlo, Regeneration of azo-dye-saturated cellulosic anion exchange resin by *Burkholderia cepacia* anaerobic dye reduction, Environ. Sci. Technol., 34 (2000) 167–172.
[23] F.-C. Wu, R.-L. Tseng, R.-S. Juang, Enhanced abilities of highly swollen chitosan beads for color removal and tyrosinase immobilization, J. Hazard. Mater., 81 (2001) 167–177.
[24] F.C. Wu, R.L. Tseng, R.S. Juang, Adsorption of dyes and humic acid from water using chitosan-encapsulated activated carbon, J. Chem. Technol. Biotechnol., 77 (2002) 1269–1279.
[25] R.-L. Tseng, F.-C. Wu, R.-S. Juang, Liquid-phase adsorption of dyes and phenols using pinewood-based activated carbons, Carbon, 41 (2003) 487–495.
[26] M.-Y. Chang, R.-S. Juang, Adsorption of tannic acid, humic acid, and dyes from water using the composite of chitosan and activated clay, J. Colloid Interface Sci., 278 (2004) 18–25.
[27] O. Ozdemir, B. Armagan, M. Turan, M.S. Celik, Comparison of the adsorption characteristics of azo-reactive dyes on mezoporous minerals, Dyes Pigm., 62 (2004) 49–60.
[28] C.-C. Wang, L.-C. Juang, T.-C. Hsu, C.-K. Lee, J.-F. Lee, F.-C. Huang, Adsorption of basic dyes onto montmorillonite, J. Colloid Interface Sci., 273 (2004) 80–86.
[29] J.-W. Lee, S.-P. Choi, R. Thiruvenkatachari, W.-G. Shim, H. Moon, Evaluation of the performance of adsorption and coagulation processes for the maximum removal of reactive dyes, Dyes Pigm., 69 (2006) 196–203.
[30] E. Lorenc-Grabowska, G. Gryglewicz, Adsorption characteristics of Congo Red on coal-based mesoporous activated carbon, Dyes Pigm., 74 (2007) 34–40.
[31] A.E. Ofomaja, Y.-S. Ho, Equilibrium sorption of anionic dye from aqueous solution by palm kernel fibre as sorbent, Dyes Pigm., 74 (2007) 60–66.
[32] M.I. Khan, S. Zafar, H.B. Ahmad, M. Hussain, Z. Shafiq, Use of morus albal leaves as bioadsorbent for the removal of congo red dye, Fresenius Environ. Bull., 24 (2015) 2251–2258.
[33] M.I. Khan, S. Zafar, M.A. Khan, F. Mumtaz, P. Prapamonthon, A.R. Buzdar, Bougainvillea glabra leaves for adsorption of congo red from wastewater, Fresenius Environ. Bull., 27 (2018) 1456–1465.
[34] M.I. Khan, S. Zafar, A.R. Buzdar, M.F. Azhar, W. Hassan, A. Aziz, Use of citrus sinensis leaves as a bioadsorbent for removal of congo red dye from aqueous solution, Fresenius Environ. Bull., 27 (2018) 4679–4688.
[35] M.I. Khan, S. Zafar, M.F. Azhar, A.R. Buzdar, W. Hassan, A. Aziz, M. Khraisheh, Leaves powder of syzgium cumini as an adsorbent for removal of congo red dye from aqueous solution, Fresenius Environ. Bull., 27 (2018) 3342–3350.
[36] J. Mittal, R. Ahmad, M.O. Ejaz, A. Mariyam, A. Mittal, A novel, eco-friendly bio-nanocomposite (Alg-Cst/Kal) for the adsorptive removal of crystal violet dye from its aqueous solutions, Int. J. Phytorem., 24 (2022) 796–807.
[37] C. Arora, S. Soni, J. Mittal, A. Mittal, B. Singh, Efficient removal of malachite green dye from aqueous solution using *Curcuma caesia* based activated carbon, Desal. Water Treat., 195 (2020) 341–352.
[38] V. Kumar, P. Saharan, A.K. Sharma, A. Umar, I. Kaushal, A. Mittal, Y. Al-Hadeethi, B. Rashad, Silver doped manganese oxide-carbon nanotube nanocomposite for enhanced dye-sequestration: isotherm studies and RSM modelling approach, Ceram. Int., 46 (2020) 10309–10319.
[39] P. Saharan, V. Kumar, J. Mittal, V. Sharma, A.K. Sharma, Efficient ultrasonic assisted adsorption of organic pollutants employing bimetallic-carbon nanocomposites, Sep. Sci. Technol., 56 (2021) 2895–2908.
[40] Y.-F. Lin, H.-W. Chen, P.-S. Chien, C.-S. Chiou, C.-C. Liu, Application of bifunctional magnetic adsorbent to adsorb metal cations and anionic dyes in aqueous solution, J. Hazard. Mater., 185 (2011) 1124–1130.
[41] M.U. Dural, L. Cavas, S.K. Papageorgiou, F.K. Katsaros, Methylene blue adsorption on activated carbon prepared from *Posidonia oceanica* (L.) dead leaves: kinetics and equilibrium studies, Chem. Eng. J., 168 (2011) 77–85.
[42] S. Karcher, A. Kornmüller, M. Jekel, Anion exchange resins for removal of reactive dyes from textile wastewaters, Water Res., 36 (2002) 4717–4724.
[43] M.I. Khan, M.H. Lashari, M. Khraisheh, S. Shahida, S. Zafar, P. Prapamonthon, A. Rehman, S. Anjum, N. Akhtar, F. Hanif, Adsorption kinetic, equilibrium and thermodynamic studies of Eosin-B onto anion exchange membrane, Desal. Water Treat., 155 (2019) 84–93.
[44] M.I. Khan, S. Akhtar, S. Zafar, A. Shaheen, M.A. Khan, R. Luque, Removal of congo red from aqueous solution by anion exchange membrane (EBTAC): adsorption kinetics and thermodynamics, Materials, 8 (2015) 4147–4161.
[45] M.I. Khan, L. Wu, A.N. Mondal, Z. Yao, L. Ge, T. Xu, Adsorption of methyl orange from aqueous solution on anion exchange membranes: adsorption kinetics and equilibrium, Membr. Water Treat., 7 (2016) 23–38.
[46] M.I. Khan, T.M. Ansari, S. Zafar, A.R. Buzdar, M.A. Khan, F. Mumtaz, P. Prapamonthon, M. Akhtar, Acid green-25 removal from wastewater by anion exchange membrane: adsorption kinetic and thermodynamic studies, Membr. Water Treat., 9 (2018) 79–85.
[47] M.A. Khan, M.I. Khan, S. Zafar, Removal of different anionic dyes from aqueous solution by anion exchange membrane, Membr. Water Treat., 8 (2017) 259–277.
[48] S.S. Ayyaril, M.I. Khan, A. Shanableh, S. Bhattacharjee, D.M. Oliveira, Fabrication of nano-activated charcoal incorporated sodium alginate-based cross-linked membrane for Rhodamine B adsorption from an aqueous solution, Desal. Water Treat., 278 (2022) 239–250.
[49] M.I. Khan, A. Shanableh, N. Elboughdiri, S. Manzoor, S. Mubeen, A. Rehman, Application of NaOH modified rice husk as a potential sorbent for removal of Congo red from an aqueous solution, Desal. Water Treat., 273 (2022) 221–235.
[50] I.W. Almanassra, M.I. Khan, A. Chatla, M.Ali Atieh, A. Shanableh, Utilization of palm leaves as an extraordinary adsorbent for the removal of Pb(II) from an aqueous solution, Desal.Water Treat., 271 (2022) 206–219.
[51] I.W. Almanassra, M.I. Khan, M.A. Atieh, A. Shanableh, Adsorption of lead ions from an aqueous solution onto NaOH-modified rice husk, Desal. Water Treat., 262 (2022) 152–167.
[52] S. Chen, Q. Yue, B. Gao, Q. Li, X. Xu, Removal of Cr(VI) from aqueous solution using modified corn stalks: characteristic, equilibrium, kinetic and thermodynamic study, Chem. Eng. J., 168 (2011) 909–917.
[53] M. Brdar, M. Šćiban, A. Takači, T. Došenović, Comparison of two and threeparameters adsorption isotherm for Cr(VI) onto Kraft lignin, Chem. Eng. J., 183 (2012) 108–111.
[54] R. Sips, Combined form of Langmuir and Freundlich equations, J. Phys. Chem., 16 (1948) 490–495.
[55] M.I. Khan, N. Elboughdiri, A. Shanableh, M.H. Lashari, S. Shahida, Application of the commercial anion exchange membrane for adsorptive removal of Eriochrome Black-T from aqueous solution, Desal. Water Treat., 252 (2022) 437–448.
[56] M.I. Khan, M.A. Khan, S. Zafar, M.N. Ashiq, M. Athar, A.M. Qureshi, M. Arshad, Kinetic, equilibrium and thermodynamic studies for the adsorption of methyl orange using new

anion exchange membrane (BII), Desal. Water Treat., 58 (2017) 285–297.
[57] S. Largergren, Zur theorie der sogenannten adsorption geloster stoffe, Kungliga Svenska Vetenskapsakademiens, Handlingar, 24 (1898) 1–39.
[58] Y.-S. Ho, G. McKay, Pseudo-second-order model for sorption processes, Process Biochem., 34 (1999) 451–465.
[59] Y.-S. Ho, Effect of pH on lead removal from water using tree fern as the sorbent, Bioresour. Technol., 96 (2005) 1292–1296.
[60] S. Zafar, N. Khalid, M. Daud, M.L. Mirza, Kinetic studies of the adsorption of thorium ions onto rice husk from aqueous media: linear and non-linear approach, Nucleus, 52 (2015) 14–19.
[61] M.C. Ncibi, Applicability of some statistical tools to predict optimum adsorption isotherm after linear and non-linear regression analysis, J. Hazard. Mater., 153 (2008) 207–212.
[62] S. Zafar, M.I. Khan, M. Khraisheh, M.H. Lashari, S. Shahida, M.F. Azhar, P. Prapamonthon, M.L. Mirza, N. Khalid, Kinetic, equilibrium and thermodynamic studies for adsorption of nickel ions onto husk of *Oryza sativa*, Desal. Water Treat., 167 (2019) 277–290.
[63] M.I. Khan, A. Shanableh, N. Nasir, S. Shahida, Adsorptive removal of methyl orange from wastewaters by the commercial anion exchange membrane EPTAC, Desal. Water Treat., 234 (2021) 245–254.
[64] S. Zafar, M.I. Khan, A. Shanableh, S. Ahmad, S. Manzoor, S. Shahida, P. Prapamonthon, S. Mubeen, A. Rehman, Adsorption of silver, thorium and nickel ions from aqueous solution onto rice husk, Desal. Water Treat., 236 (2021) 108–122.